

# Effects of isospin and momentum dependent interactions on liquid-gas phase transition in hot asymmetric nuclear matter

Jun Xu,<sup>1</sup> Lie-Wen Chen,<sup>1,2</sup> Bao-An Li,<sup>3</sup> and Hong-Ru Ma<sup>1</sup>

<sup>1</sup>*Institute of Theoretical Physics, Shanghai Jiao Tong University, Shanghai 200240, China*

<sup>2</sup>*Center of Theoretical Nuclear Physics, National Laboratory of Heavy-Ion Accelerator, Lanzhou, 730000, China*

<sup>3</sup>*Department of Physics, Texas A&M University-Commerce, Commerce, TX 75429-3011, USA*

The liquid-gas phase transition in hot neutron-rich nuclear matter is investigated within a self-consistent thermal model using an isospin and momentum dependent interaction (MDI) constrained by the isospin diffusion data in heavy-ion collisions, a momentum-independent interaction (MID), and an isoscalar momentum-dependent interaction (eMDYI). The boundary of the phase-coexistence region is shown to be sensitive to the density dependence of the nuclear symmetry energy with a softer symmetry energy giving a higher critical pressure and a larger area of phase-coexistence region. Compared with the momentum-independent MID interaction, the isospin and momentum-dependent MDI interaction is found to increase the critical pressure and enlarge the area of phase-coexistence region. For the isoscalar momentum-dependent eMDYI interaction, a limiting pressure above which the liquid-gas phase transition cannot take place has been found and it is shown to be sensitive to the stiffness of the symmetry energy.

PACS numbers: 21.65.+f, 21.30.Fe, 24.10.Pa, 64.10.+h

The van der Waals behavior of the nucleon-nucleon interaction is expected to lead to the so-called liquid-gas (LG) phase transition in nuclear matter. Since the early work, see, e.g., Refs. [1, 2, 3, 4], many investigations have been carried out to explore properties of the nuclear LG phase transition both experimentally and theoretically over the last three decades. For a recent review, see, e.g., Refs. [5, 6, 7]. Most of these studies focused on investigating features of the LG phase transition in symmetric nuclear matter. Recent progress in experiments with radioactive beams provided us a great opportunity to explore more extensively the LG phase transition in isospin-asymmetric nuclear matter. New features of the LG phase transition in asymmetric nuclear matter are expected. In particular, in an asymmetric nuclear matter, there are two components of protons and neutrons, and two conserved charges of baryon number and the third component of isospin, and the LG phase transition was suggested to be of second order [8]. This suggestion together with the need to understand better properties of asymmetric nuclear matter relevant for both nuclear physics and astrophysics have stimulated a lot of work recently, see, e.g., Refs. [9, 10, 11, 12, 13, 14, 15, 16, 17, 18]. While significant progress has been made recently, many interesting questions about the nature of the LG phase transition in asymmetric nuclear matter remain open. Some of these questions can be traced back to our poor understanding about the isovector nuclear interaction and the density dependence of the nuclear symmetry energy [7, 19, 20]. Fortunately, recent analyses of the isospin diffusion data in heavy-ion reactions have allowed us to put a stringent constraint on the symmetry energy of neutron-rich matter at sub-normal densities [21, 22, 23]. It is therefore interesting to investigate how the constrained symmetry energy may allow us to better understand the LG phase transition in asymmetric nuclear matter. More-

over, both the isovector (i.e., the nuclear symmetry potential) and isoscalar parts of the single nucleon potential should be momentum dependent due to the non-locality of nucleon-nucleon interaction and the Pauli exchange effects in many-fermion systems. However, effects of the momentum-dependent interactions on the LG phase transition in asymmetric nuclear matter have received so far little theoretical attention. A timely remedy of the situation is imperative given the experimental studies underway or planned at various radioactive beam facilities.

In the present work, we study effects of isospin and momentum dependent interactions on the LG phase transition in hot neutron-rich nuclear matter within a self-consistent thermal model using three different interactions. The first one is the isospin and momentum dependent MDI interaction constrained by the isospin diffusion data in heavy-ion collisions. The second one is a momentum-independent interaction (MID) which leads to a fully momentum independent single nucleon potential, and the third one is an isoscalar momentum-dependent interaction (eMDYI) in which the isoscalar part of the single nucleon potential is momentum dependent but the isovector part of the single nucleon potential is momentum independent.

In the isospin and momentum-dependent MDI interaction, the potential energy density  $V_{\text{MDI}}(\rho, T, \delta)$  of a thermally equilibrated asymmetric nuclear matter at total density  $\rho$ , temperature  $T$  and isospin asymmetry  $\delta$  is expressed as follows [22, 24],

$$\begin{aligned} V_{\text{MDI}}(\rho, T, \delta) = & \frac{A_u \rho_n \rho_p}{\rho_0} + \frac{A_l}{2\rho_0} (\rho_n^2 + \rho_p^2) + \frac{B}{\sigma + 1} \frac{\rho^{\sigma+1}}{\rho_0^\sigma} \\ & \times (1 - x\delta^2) + \frac{1}{\rho_0} \sum_{\tau, \tau'} C_{\tau, \tau'} \\ & \times \int \int d^3p d^3p' \frac{f_\tau(\vec{r}, \vec{p}) f_{\tau'}(\vec{r}, \vec{p}')}{1 + (\vec{p} - \vec{p}')^2 / \Lambda^2}. \end{aligned} \quad (1)$$

In the mean field approximation, Eq. (1) leads to the following single particle potential for a nucleon with momentum  $\vec{p}$  and isospin  $\tau$  in the thermally equilibrated asymmetric nuclear matter [22, 24]

$$\begin{aligned}
U_{\text{MDI}}(\rho, T, \delta, \vec{p}, \tau) = & A_u(x) \frac{\rho_{-\tau}}{\rho_0} + A_l(x) \frac{\rho_\tau}{\rho_0} + B \left( \frac{\rho}{\rho_0} \right)^\sigma \\
& \times (1 - x\delta^2) - 8\tau x \frac{B}{\sigma + 1} \frac{\rho^{\sigma-1}}{\rho_0^\sigma} \delta \rho_{-\tau} \\
& + \frac{2C_{\tau,\tau}}{\rho_0} \int d^3p' \frac{f_\tau(\vec{r}, \vec{p}')}{1 + (\vec{p} - \vec{p}')^2/\Lambda^2} \\
& + \frac{2C_{\tau,-\tau}}{\rho_0} \int d^3p' \frac{f_{-\tau}(\vec{r}, \vec{p}')}{1 + (\vec{p} - \vec{p}')^2/\Lambda^2} \quad (2)
\end{aligned}$$

In the above  $\tau = 1/2$  ( $-1/2$ ) for neutrons (protons) and  $f_\tau(\vec{r}, \vec{p})$  is the phase space distribution function at coordinate  $\vec{r}$  and momentum  $\vec{p}$ . The detailed values of the parameters  $\sigma, A_u(x), A_l(x), B, C_{\tau,\tau}, C_{\tau,-\tau}$  and  $\Lambda$  can be found in Refs. [22, 24] and have been assumed to be temperature independent here. The isospin and momentum-dependent MDI interaction gives the binding energy per nucleon of  $-16$  MeV, incompressibility  $K_0 = 211$  MeV and the symmetry energy of  $31.6$  MeV for cold symmetric nuclear matter at saturation density  $\rho_0 = 0.16 \text{ fm}^{-3}$  [24]. The different  $x$  values in the MDI interaction are introduced to vary the density dependence of the nuclear symmetry energy while keeping other properties of the nuclear equation of state fixed [22]. We note that the MDI interaction has been extensively used in the transport model for studying isospin effects in intermediate energy heavy-ion collisions induced by neutron-rich nuclei [22, 23, 25, 26, 27, 28, 29, 30]. In particular, the isospin diffusion data from NSCL/MSU have constrained the value of  $x$  to be between 0 and  $-1$  for nuclear matter densities less than about  $1.2\rho_0$  [22, 23], we will thus in the present work consider the two values of  $x = 0$  and  $x = -1$ . We note that the zero-temperature symmetry energy for the MDI interaction with  $x = 0$  and  $-1$  can be parameterized, respectively, as  $31.6(\rho/\rho_0)^{0.69}$  MeV and  $31.6(\rho/\rho_0)^{1.05}$  MeV [22], and thus  $x = 0$  gives a softer symmetry energy while  $x = -1$  gives a stiffer symmetry energy.

In the momentum-independent MID interaction, the potential energy density  $V_{\text{MID}}(\rho, \delta)$  of a thermally equilibrated asymmetric nuclear matter at total density  $\rho$  and isospin asymmetry  $\delta$  can be written as

$$V_{\text{MID}}(\rho, \delta) = \frac{\alpha}{2} \frac{\rho^2}{\rho_0} + \frac{\beta}{1 + \gamma} \frac{\rho^{1+\gamma}}{\rho_0^\gamma} + \rho E_{\text{sym}}^{\text{pot}}(\rho, x) \delta^2. \quad (3)$$

The parameters  $\alpha, \beta$  and  $\gamma$  are determined by the incompressibility  $K_0$  of cold symmetric nuclear matter at

saturation density  $\rho_0$  [9]

$$\alpha = -29.81 - 46.90 \frac{K_0 + 44.73}{K_0 - 166.32} \text{ (MeV)} \quad (4)$$

$$\beta = 23.45 \frac{K_0 + 255.78}{K_0 - 166.32} \text{ (MeV)} \quad (5)$$

$$\gamma = \frac{K_0 + 44.73}{211.05} \quad (6)$$

and  $K_0$  is again set to be  $211$  MeV as in the MDI interaction. To fit the MDI interaction at zero temperature, the potential part of the symmetry energy  $E_{\text{sym}}^{\text{pot}}(\rho, x)$  is parameterized by [22]

$$E_{\text{sym}}^{\text{pot}}(\rho, x) = F(x) \frac{\rho}{\rho_0} + [18.6 - F(x)] \left( \frac{\rho}{\rho_0} \right)^{G(x)} \quad (7)$$

with  $F(x = 0) = 129.981$  MeV,  $G(x = 0) = 1.059$ ,  $F(x = -1) = 3.673$  MeV, and  $G(x = -1) = 1.569$ . We note that the MID interaction reproduces very well the EOS of isospin-asymmetric nuclear matter with the MDI interaction at zero temperature for both  $x = 0$  and  $x = -1$ . The single nucleon potential in the MID interaction can be directly obtained as

$$U_{\text{MID}}(\rho, \delta, \tau) = \alpha \frac{\rho}{\rho_0} + \beta \left( \frac{\rho}{\rho_0} \right)^\gamma + U^{\text{asy}}(\rho, \delta, \tau), \quad (8)$$

with

$$\begin{aligned}
U^{\text{asy}}(\rho, \delta, \tau) = & \left[ 4F(x) \frac{\rho}{\rho_0} + 4(18.6 - F(x)) \left( \frac{\rho}{\rho_0} \right)^{G(x)} \right] \tau \delta \\
& + (18.6 - F(x))(G(x) - 1) \left( \frac{\rho}{\rho_0} \right)^{G(x)} \delta^2. \quad (9)
\end{aligned}$$

Therefore, the single nucleon potential in the MID interaction is fully momentum-independent. It also leads to the fact that the potential energy density and the single nucleon potential in the MID interaction are independent of the temperature.

The momentum-dependent part in the MDI interaction is also isospin dependent while the MID interaction is fully momentum independent. In order to see the effect of the momentum dependence of the isovector part of the single nucleon potential (nuclear symmetry potential), we can introduce an isoscalar momentum-dependent interaction, called extended MDYI (eMDYI) interaction since it has the same functional form as the well-known MDYI interaction for symmetric nuclear matter [31]. In the eMDYI interaction, the potential energy density  $V_{\text{eMDYI}}(\rho, T, \delta)$  of a thermally equilibrated asymmetric nuclear matter at total density  $\rho$ , temperature  $T$  and isospin asymmetry  $\delta$  can be written as

$$\begin{aligned}
V_{\text{eMDYI}}(\rho, T, \delta) = & \frac{A}{2} \frac{\rho^2}{\rho_0} + \frac{B}{1 + \sigma} \frac{\rho^{1+\sigma}}{\rho_0^\sigma} \\
& + \frac{C}{\rho_0} \int \int d^3p d^3p' \frac{f_0(\vec{r}, \vec{p}) f_0(\vec{r}, \vec{p}')}{1 + (\vec{p} - \vec{p}')^2/\Lambda^2} \\
& + \rho E_{\text{sym}}^{\text{pot}}(\rho, x) \delta^2. \quad (10)
\end{aligned}$$

Here  $f_0(\vec{r}, \vec{p})$  is the phase space distribution function of *symmetric nuclear matter* at total density  $\rho$  and temperature  $T$ .  $E_{sym}^{pot}(\rho, x)$  has the same expression as Eq. (7). We set  $A = \frac{A_u + A_l}{2}$  and  $C = \frac{C_{\tau, -\tau} + C_{\tau, \tau}}{2}$ , and  $B$ ,  $\sigma$  and  $\Lambda$  have the same values as in the MDI interaction, so that the eMDYI interaction gives the same EOS of asymmetric nuclear matter as the MDI interaction at zero temperature for both  $x = 0$  and  $x = -1$ . The single nucleon potential in the eMDYI interaction can be obtained as

$$U_{\text{eMDYI}}(\rho, T, \delta, \vec{p}, \tau) = U^0(\rho, T, \vec{p}) + U^{\text{asy}}(\rho, \delta, \tau), \quad (11)$$

where

$$U^0(\rho, T, \vec{p}) = A \frac{\rho}{\rho_0} + B \left( \frac{\rho}{\rho_0} \right)^\sigma + \frac{2C}{\rho_0} \int d^3 p' \frac{f_0(\vec{r}, \vec{p}')}{1 + (\vec{p} - \vec{p}')^2 / \Lambda^2} \quad (12)$$

and  $U^{\text{asy}}(\rho, \delta, \tau)$  is the same as Eq. (9) which implies that the symmetry potential is identical for the eMDYI and MID interactions. Therefore, in the eMDYI interaction, the isoscalar part of the single nucleon potential is momentum dependent but the nuclear symmetry potential is not. For symmetric nuclear matter, the single nucleon potential in the eMDYI interaction is exactly the same as that in the MDI interaction. We note that the same strategy has been used to study the momentum dependence effects in heavy-ion collisions in a previous work [26].

At zero temperature,  $f_\tau(\vec{r}, \vec{p}) = \frac{2}{h^3} \Theta(p_f(\tau) - p)$  and all the integrals in above expressions can be calculated analytically, while at a finite temperature  $T$ , the phase space distribution function becomes the Fermi distribution

$$f_\tau(\vec{r}, \vec{p}) = \frac{2}{h^3} \frac{1}{\exp\left(\frac{p^2}{2m_\tau} + U_\tau - \mu_\tau\right) + 1} \quad (13)$$

where  $\mu_\tau$  is the proton or neutron chemical potential and can be determined from

$$\rho_\tau = \int f_\tau(\vec{r}, \vec{p}) d^3 p. \quad (14)$$

In the above,  $m_\tau$  is the proton or neutron mass and  $U_\tau$  is the proton or neutron single nucleon potential in different interactions. From a self-consistency iteration scheme [31, 32], the chemical potential  $\mu_\tau$  and the distribution function  $f_\tau(\vec{r}, \vec{p})$  can be determined numerically.

From the chemical potential  $\mu_\tau$  and the distribution function  $f_\tau(\vec{r}, \vec{p})$ , the energy per nucleon  $E(\rho, T, \delta)$  can be obtained as

$$E(\rho, T, \delta) = \frac{1}{\rho} \left[ V(\rho, T, \delta) + \sum_\tau \int d^3 p \frac{p^2}{2m_\tau} f_\tau(\vec{r}, \vec{p}) \right]. \quad (15)$$

Furthermore, we can obtain the entropy per nucleon  $S_\tau(\rho, T, \delta)$  as

$$S_\tau(\rho, T, \delta) = -\frac{8\pi}{\rho h^3} \int_0^\infty p^2 [n_\tau \ln n_\tau + (1 - n_\tau) \ln(1 - n_\tau)] dp \quad (16)$$

with the occupation probability

$$n_\tau = \frac{1}{\exp\left(\frac{p^2}{2m_\tau} + U_\tau - \mu_\tau\right) + 1}. \quad (17)$$

Finally, the pressure  $P(\rho, T, \delta)$  can be calculated from the thermodynamic relation

$$P(\rho, T, \delta) = \left[ T \sum_\tau S_\tau(\rho, T, \delta) - E(\rho, T, \delta) \right] \rho + \sum_\tau \mu_\tau \rho_\tau. \quad (18)$$

With the above theoretical models, we can now study the LG phase transition in hot asymmetric nuclear matter. The phase coexistence is governed by the Gibbs conditions and for the asymmetric nuclear matter two-phase coexistence equations are

$$\mu_i^L(T, \rho_i^L) = \mu_i^G(T, \rho_i^G), (i = n \text{ and } p) \quad (19)$$

$$P_i^L(T, \rho_i^L) = P_i^G(T, \rho_i^G), (i = n \text{ or } p) \quad (20)$$

where  $L$  and  $G$  stand for liquid phase and gas phase, respectively. The chemical stability condition is given by

$$\left( \frac{\partial \mu_n}{\partial \delta} \right)_{P, T} > 0 \text{ and } \left( \frac{\partial \mu_p}{\partial \delta} \right)_{P, T} < 0. \quad (21)$$

The Gibbs conditions (19) and (20) for phase equilibrium require equal pressures and chemical potentials for two phases with different concentrations. For a fixed pressure, the two solutions thus form the edges of a rectangle in the proton and neutron chemical potential isobars as a function of isospin asymmetry  $\delta$  and can be found by means of the geometrical construction method [8, 11].

The solid curves shown in Fig. 1 are the proton and neutron chemical potential isobars as a function of the isospin asymmetry  $\delta$  at a fixed temperature  $T = 10$  MeV and pressure  $P = 0.090$  MeV/fm<sup>3</sup> by using the MDI and MID interactions with  $x = 0$  and  $x = -1$ . The resulting rectangles from the geometrical construction are also shown by dotted lines in Fig. 1. For each interaction, the two different values of  $\delta$  correspond to two different phases with different densities and the lower density phase (with larger  $\delta$  value) defines a gas phase while the higher density phase (with smaller  $\delta$  value) defines a liquid phase. Collecting all such pairs of  $\delta(T, P)$  and  $\delta'(T, P)$  thus forms the binodal surface. From Fig. 1, one can see that different interactions give different shapes for the chemical potential isobar. When the pressure increases and approaches the critical pressure  $P_C$ , an inflection point will appear for proton and neutron chemical potential isobars, i.e.,

$$\left( \frac{\partial \mu}{\partial \delta} \right)_{P_C, T} = \left( \frac{\partial^2 \mu}{\partial \delta^2} \right)_{P_C, T} = 0. \quad (22)$$

Above the critical pressure, the chemical potential of neutrons (protons) increases (decreases) monotonically with

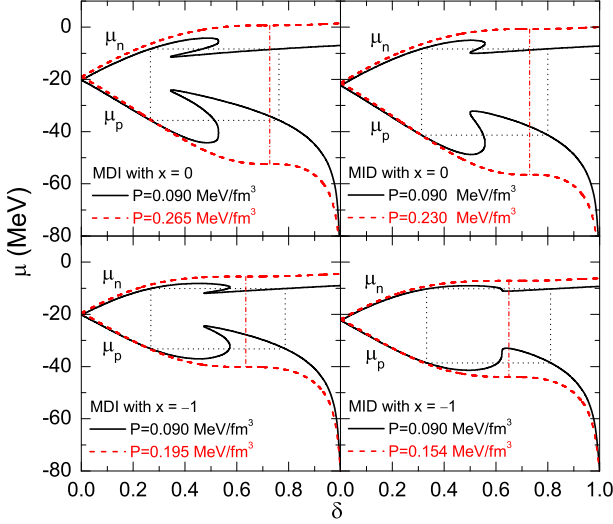


FIG. 1: (Color online) The chemical potential isobar as a function of the isospin asymmetry  $\delta$  at  $T = 10$  MeV in the MDI and MID interactions with  $x = 0$  and  $x = -1$ . The geometrical construction used to obtain the isospin asymmetries and chemical potentials in the two coexisting phases is also shown.

$\delta$  and the chemical instability disappears. In Fig. 1, we also show the chemical potential isobar at the critical pressure by the dashed curves. At the critical pressure, the rectangle is degenerated to a line vertical to the  $\delta$  axis as shown by dash-dotted lines in Fig. 1. The values of the critical pressure are 0.265, 0.230, 0.195 and 0.154 MeV/fm<sup>3</sup> for the MDI interaction with  $x = 0$ , MID interaction with  $x = 0$ , MDI interaction with  $x = -1$  and MID interaction with  $x = -1$ , respectively. It is interesting to see that the different interactions give different values of the critical pressure. Especially, the stiffer symmetry energy ( $x = -1$ ) gives a smaller critical pressure while the inclusion of the momentum dependence in the interaction (MDI) gives a larger critical pressure.

In Fig. 2, we show the section of the binodal surface at  $T = 10$  MeV for the MDI and MID interactions with  $x = 0$  and  $x = -1$ . On the left side of the binodal surface there only exists a liquid phase and on the right side only a gas phase exists. In the region of “filet mignon” is the coexistence phase of liquid phase and gas phase. Interestingly, we can see from Fig. 2 that the stiffer symmetry energy ( $x = -1$ ) significantly lowers the critical point (CP) and makes the maximal asymmetry (MA) a little smaller. Meanwhile, the momentum dependence in the interaction (MDI) lifts the CP in a larger amount, while it seems to have no effects on the MA point. In addition, just as expected, the value of  $x$  does not affect the equal concentration (EC) point while the momentum dependence lifts it slightly (by about 0.005 MeV/fm<sup>3</sup>). These features clearly indicate that the critical pressure and the area of phase-coexistence region in hot asymmetric nuclear matter is very sensitive

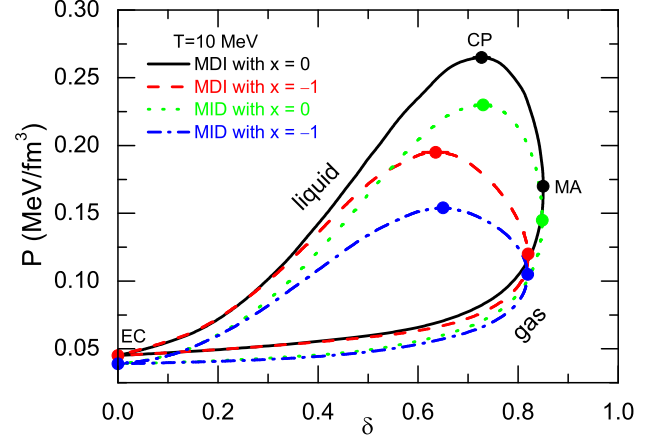


FIG. 2: (Color online) The section of binodal surface at  $T = 10$  MeV in the MDI and MID interactions with  $x = 0$  and  $x = -1$ . The critical point (CP), the points of equal concentration (EC) and maximal asymmetry (MA) are also indicated.

to the stiffness of the symmetry energy with a softer symmetry energy giving a higher critical pressure and a larger area of phase-coexistence region. Meanwhile, the momentum dependence in the interaction significantly increases the critical pressure and enlarges the area of phase-coexistence region.

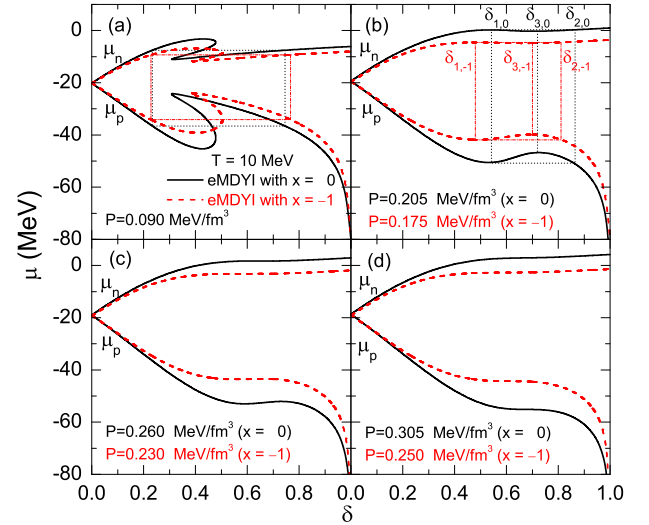


FIG. 3: (Color online) The chemical potential isobar as a function of isospin asymmetry  $\delta$  at  $T = 10$  MeV in the eMDYI interaction with  $x = 0$  and  $x = -1$ .

We now turn to the case of the eMDYI interaction. In the eMDYI interaction, the resulting single nucleon potential is momentum dependent but its momentum dependence is isospin-independent. Comparing the results with those of the MDI interaction, we can extract infor-

mation about the effects of the momentum dependence of the symmetry potential while the effects of the momentum dependence of the isoscalar part of the single nucleon potential can be studied by comparing the results with those of the MDI interaction. Shown in Fig. 3 is the chemical potential isobar as a function of the isospin asymmetry  $\delta$  at  $T = 10$  MeV by using the eMDYI interaction with  $x = 0$  and  $x = -1$ . Compared with the results from the MDI and MID interactions, the main difference is that the left (and right) extrema of  $\mu_n$  and  $\mu_p$  do not correspond to a same  $\delta$  but they do for the MDI and MID interactions as shown in Fig. 1. In particular, for the eMDYI interaction, the chemical potentials of protons and neutrons are seen to exhibit asynchronous variation with pressure, i.e., the chemical potential of neutrons increase more rapidly with pressure than that of protons. This asynchronous variation is uniquely determined by the special momentum dependence in the eMDYI interaction within the present self-consistent thermal model. Actually, it is this asynchronous variation that leads to the fact that the left (and right) extrema of  $\mu_n$  and  $\mu_p$  correspond to different values of  $\delta$ .

At lower pressures, for example,  $P = 0.090$  MeV/fm<sup>3</sup> as shown in Fig. 3 (a), the rectangle can be accurately constructed and thus the Gibbs conditions (19) and (20) have two solutions. Due to the asynchronous variation of  $\mu_n$  and  $\mu_p$  with pressure, we will get a limiting pressure  $P_{\text{lim}}$  above which no rectangle can be constructed and the coexistence equations (19) and (20) have no solution. Fig. 3 (b) shows the case at the limiting pressure with  $P_{\text{lim}} = 0.205$  and  $0.175$  MeV/fm<sup>3</sup> for  $x = 0$  and  $x = -1$ , respectively. In this limit case, we note that for  $x = 0$  the left edge of the rectangle actually corresponds to the left extremum of  $\mu_p$  and the pair  $\delta_{1,0} = 0.600$  and  $\delta_{2,0} = 0.750$  form the two edges of the rectangle (the end of the binodal surface) while for  $x = -1$  it corresponds to the left extremum of  $\mu_n$  and the pair  $\delta_{1,-1} = 0.480$  and  $\delta_{2,-1} = 0.811$  form the two edges of the rectangle. The  $\delta_{3,0} = 0.720$  and  $\delta_{3,-1} = 0.700$  indicated in Fig. 3 (b) correspond to the maximum of  $\mu_p$  for  $x = 0$  and  $x = -1$ , respectively. With increasing pressure, namely, at  $P = 0.260$  and  $0.230$  MeV/fm<sup>3</sup> for  $x = 0$  and  $x = -1$ , respectively,  $\mu_n$  passes through an inflection point while  $\mu_p$  still has a chemically unstable region and this case is shown in Fig. 3 (c). When the pressure is further increased to  $P = 0.305$  and  $0.250$  MeV/fm<sup>3</sup> for  $x = 0$  and  $x = -1$ , respectively, as shown in Fig. 3 (d),  $\mu_p$  passes through an inflection point while  $\mu_n$  increases monotonically with  $\delta$ . These features indicate that the asynchronous variation of  $\mu_n$  and  $\mu_p$  with pressure also depends on the value of  $x$ .

Fig. 4 displays the section of the binodal surface at  $T = 10$  MeV by using the eMDYI interaction with  $x = 0$  and  $x = -1$ . We can see that the curve is cut off at the limiting pressure with  $P_{\text{lim}} = 0.205$  and  $0.175$  MeV/fm<sup>3</sup> for  $x = 0$  and  $x = -1$ , respectively. It is interesting to see that for  $x = -1$  there is an bending point at  $\delta_{\text{max},-1} = 0.823$ , but for  $x = 0$  there is

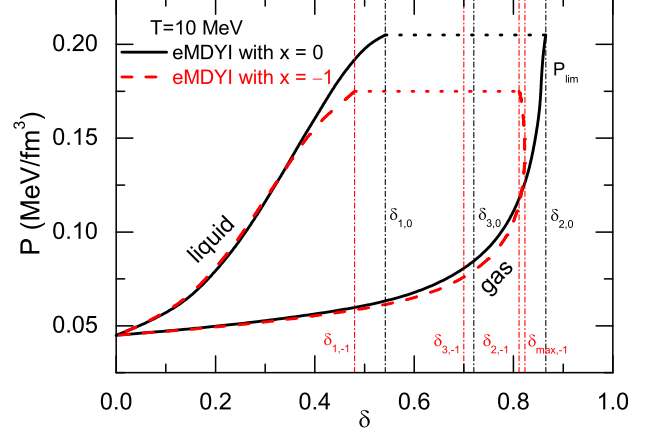


FIG. 4: (Color online) The section of binodal surface at  $T = 10$  MeV in the eMDYI interaction with  $x = 0$  and  $x = -1$ .  $P_{\text{lim}}$  represents the limiting pressure and  $\delta_{i,j}$ 's are discussed in the text.

no such point. For  $x = -1$  the situation is similar to that found in Ref. [11] using different models and the isospin asymmetry  $\delta$  can be divided into four regions:  $[0, \delta_{1,-1}]$ ,  $[\delta_{1,-1}, \delta_{3,-1}]$ ,  $[\delta_{3,-1}, \delta_{2,-1}]$  and  $[\delta_{2,-1}, \delta_{\text{max},-1}]$ . In the first region  $[0, \delta_{1,-1}]$ , the system begins at gas phase, experiences a LG phase transition and ends at liquid phase. In the second region  $[\delta_{1,-1}, \delta_{3,-1}]$ , it begins at gas phase, enters a two-phase region and becomes unstable at the limiting pressure, as chemical instability condition Eq. (21) is destroyed in this region. In the third region  $[\delta_{3,-1}, \delta_{2,-1}]$ , the system will end in a stable phase as Eq. (21) is satisfied in this region. In the fourth region  $[\delta_{2,-1}, \delta_{\text{max},-1}]$ , the system enters and leaves the two-phase region on the same branch, so it remains in the gas phase at the end. For  $x = 0$ , the situation is simpler and  $\delta$  can be divided into three regions:  $[0, \delta_{1,0}]$ ,  $[\delta_{1,0}, \delta_{3,0}]$  and  $[\delta_{3,0}, \delta_{2,0}]$ . The discussion is similar to that of the first, second and third regions in the case of  $x = -1$ .

From Fig. 4, we can also see that the limiting pressure and the area of phase-coexistence region are still sensitive to the stiffness of the symmetry energy with a softer symmetry energy ( $x = 0$ ) giving a higher limit pressure and a larger area of phase-coexistence region. Comparing the results of the MDI and MID interactions shown in Fig. 2, we can see that for pressures lower than the limiting pressure, the binodal surface from the eMDYI interaction is similar to that from the MDI interaction. This feature implies that the momentum dependence of the symmetry potential has little influence on the LG phase transition in hot asymmetric nuclear matter while the momentum dependence of the isoscalar single nucleon potential significantly enlarges the area of phase-coexistence region for pressures lower than the limiting pressure. For pressures above the limiting pressure, the momentum dependence of both the isoscalar and isovector single nucleon

potentials becomes important.

In summary, we have studied the liquid-gas phase transition in hot neutron-rich nuclear matter within a self-consistent thermal model using three different nuclear effective interactions, namely, the isospin and momentum dependent MDI interaction constrained by the isospin diffusion data in heavy-ion collisions, the momentum-independent MID interaction, and the isoscalar momentum-dependent eMDYI interaction. At zero temperature, the above three interactions give the same EOS for asymmetric nuclear matter. The MDI interaction is realistic, while the MID and eMDYI interactions are only used as references in order to explore effects of the isospin and momentum dependence on the liquid-gas phase transition. Since the symmetry energy corresponding to the MDI interaction has been already restricted within a narrow range by the isospin diffusion data in heavy-ion collisions, predictions using the MDI interaction thus allow us to constrain the liquid-gas phase boundary in asymmetric nuclear matter.

Comparing calculations with the three interactions, we find that the boundary of the phase-coexistence region is very sensitive to the density dependence of the nuclear symmetry energy. A softer symmetry energy leads to a higher critical pressure and a larger area of the phase-coexistence region. On the other hand, compared with the momentum-independent MID interaction, the isospin and momentum-dependent MDI interaction increases the critical pressure and enlarge the area of phase-coexistence

region. For the isoscalar momentum-dependent eMDYI interaction, there is a limiting pressure above which the liquid-gas phase transition cannot take place due to the asynchronous variations of the nucleon chemical potentials with pressure. Comparing the results of the eMDYI interaction with those of the MDI and MID interactions, we find that, for pressures lower than the limiting pressure, the momentum dependence of the symmetry potential has little influence on the liquid-gas phase transition in hot asymmetric nuclear matter. While the momentum dependence of the isoscalar single nucleon potential significantly enlarges the area of phase-coexistence region. For pressures above the limiting pressure, the momentum dependence of both the isoscalar and isovector single nucleon potentials becomes important.

### Acknowledgments

This work was supported in part by the National Natural Science Foundation of China under Grant Nos. 10334020, 10575071, and 10675082, MOE of China under project NCET-05-0392, Shanghai Rising-Star Program under Grant No. 06QA14024, the SRF for ROCS, SEM of China, the US National Science Foundation under Grant No. PHY-0652548 and the Research Corpora-

- 
- [1] D. Q. Lamb, J. M. Lattimer, C. J. Pethick, and D. G. Ravenhall, Phys. Rev. Lett. **41**, 1623 (1978).
  - [2] J.E. Finn et al., Phys. Rev. Lett. **49**, 1321 (1982).
  - [3] G.F. Bertsch and P.J. Siemens, Phys. Lett. **B126**, 9 (1983).
  - [4] H. Jaquez, A. Z. Mekjian, and L. Zamick, Phys. Rev. C **27**, 2782 (1983); *ibid.* C **29**, 2067 (1984).
  - [5] Ph. Chomaz, M. Colonna, and J. Randrup, Phys. Rep. **389**, 263 (2004).
  - [6] C.B. Das, S. Das Gupta, W.G. Lynch, A.Z. Mekjian, and M.B. Tsang, Phys. Rep. **406**, 1 (2005).
  - [7] *Dynamics and Thermodynamics with Nucleonic Degrees of Freedom*, Eds. Ph. Chomaz, F. Gulminelli, W. Trautmann and S.J. Yennello, Springer, (2006).
  - [8] H. Müller and B.D. Serot, Phys. Rev. C **52**, 2072 (1995).
  - [9] B.A. Li and C.M. Ko, Nucl. Phys. **A618**, 498 (1997).
  - [10] P. Wang, Phys. Rev. C **61**, 054904 (2000).
  - [11] W.L. Qian, R.K. Su, and P. Wang, Phys. Lett. **B491**, 90 (2000).
  - [12] S.J. Lee and A. Z. Mekjian, Phys. Rev. C **63**, 044605 (2001).
  - [13] B.A. Li, A.T. Sustich, M. Tilley, and B. Zhang, Phys. Rev. C **64**, 051303(R) (2001).
  - [14] J.B. Natowitz et al., Phys. Rev. Lett. **89**, 212701 (2002).
  - [15] B.A. Li, A.T. Sustich, M. Tilley, and B. Zhang, Nucl. Phys. **A699**, 493 (2002).
  - [16] P. Chomaz and J. Margueron, Nucl. Phys. **A722**, 315c (2003); J. Margueron and P. Chomaz, Phys. Rev. C **67**, 041602(R) (2003).
  - [17] T. Sil, S.K. Samaddar, J.N. De, and S. Shlomo, Phys. Rev. C **69**, 014602 (2004).
  - [18] C. Ducoin, P. Chomaz, and F. Gulminelli, Nucl. Phys. **A771**, 68 (2006); *ibid.* **A781**, 407 (2007).
  - [19] B.A. Li, C.M. Ko, and W. Bauer, topical review, Int. Jour. Mod. Phys. E **7**, 147 (1998).
  - [20] *Isospin Physics in Heavy-Ion Collisions at Intermediate Energies*, Eds.. Bao-An Li and W. Udo Schröder (Nova Science Publishers, Inc, New York, 2001).
  - [21] M.B. Tsang et al., Phys. Rev. Lett. **92**, 062701 (2004).
  - [22] L.W. Chen, C.M. Ko, and B.A. Li, Phys. Rev. Lett. **94**, 032701 (2005) [arXiv:nucl-th/0407032].
  - [23] B.A. Li and L.W. Chen, Phys. Rev. C **72**, 064611 (2005).
  - [24] C. B. Das, S. Das Gupta, C. Gale and B.A. Li, Phys. Rev. C **67**, 034611 (2003).
  - [25] B.A. Li, C. B. Das, S. Das Gupta, and C. Gale, Phys. Rev. C **69**, 011603(R) (2004); Nucl. Phys. **A735**, 563 (2004).
  - [26] L.W. Chen, C.M. Ko, and B.A. Li, Phys. Rev. C **69**, 054606 (2004).
  - [27] B.A. Li, G.C. Yong, and W. Zuo, Phys. Rev. C **71**, 014608 (2005); *ibid.* C **71**, 044604 (2005).
  - [28] B.A. Li, L.W. Chen, G.C. Yong, and W. Zuo, Phys. Lett. **B634**, 378 (2006).
  - [29] G.C. Yong, B.A. Li, L.W. Chen, and W. Zuo, Phys. Rev. C **73**, 034603 (2006).
  - [30] G.C. Yong, B.A. Li, and L.W. Chen, Phys. Rev. C **74**,

- 064617 (2006) [arXiv:nucl-th/0606003].
- [31] C. Gale, G.M. Welke, M. Prakash, S.J. Lee, and S. Das Gupta, Phys. Rev. C **41**, 1545 (1990).
- [32] J. Xu, L.W. Chen, B.A. Li, and H.R. Ma, Phys. Rev. C **75**, 014607 (2007) [arXiv:nucl-th/0609035].